

DISCOVERY OF SUB- TO SUPERLUMINAL MOTIONS IN THE M87 JET: AN IMPLICATION OF ACCELERATION FROM SUB-RELATIVISTIC TO RELATIVISTIC SPEEDS

KEIICHI ASADA¹, MASANORI NAKAMURA¹, AKIHIRO DOI², HIROSHI NAGAI³, AND MAKOTO INOUE¹

¹ Institute of Astronomy and Astrophysics, Academia Sinica, P.O. Box 23-141, Taipei 10617, Taiwan; asada@asiaa.sinica.edu.tw, nakamura@asiaa.sinica.edu.tw

² Institute of Space and Astronautical Science, Japan Aerospace Exploration Agency, 3-1-1 Yoshinodai, Chuou-ku, Sagami-hara, Kanagawa 229-8510, Japan

³ National Astronomical Observatory of Japan, 2-21-1, Osawa, Tokyo 81-8588, Japan

Received 2013 August 29; accepted 2013 November 10; published 2013 December 23

ABSTRACT

The velocity field of the M87 jet from milli-arcsecond (mas) to arcsecond scales is extensively investigated together with new radio images taken from European VLBI Network (EVN) observations. We detected proper motions of components located at between 160 mas from the core and the HST-1 complex for the first time. Newly derived velocity fields exhibit a systematic increase from sub- to superluminal speeds in the upstream of HST-1. If we assume that the observed velocities reflect the bulk flow, here we suggest that the M87 jet may be gradually accelerated through a distance of 10^6 times the Schwarzschild radius of the supermassive black hole. The acceleration zone is co-spatial with the jet parabolic region, which is interpreted as the collimation zone of the jet. The acceleration and collimation take place simultaneously, which we suggest is characteristic of magnetohydrodynamic flows. The distribution of the velocity field has a peak at HST-1, which is considered as the site of over-collimation, and shows a deceleration downstream of HST-1 where the jet is conical. Our interpretation of the velocity map in the M87 jet provides a hypothesis for active galactic nuclei which suggests that the acceleration and collimation zone of relativistic jets extends over the whole scale within the sphere of influence of the supermassive black hole.

Key words: galaxies: active – galaxies: individual (M87) – galaxies: jets

Online-only material: color figures

1. INTRODUCTION

Understanding the acceleration mechanism of relativistic jets is one of the long-standing issues in high energy astrophysics. Observations of proper motion with a high angular resolution have been established as a useful tool to trace the kinematics of relativistic jets. For such proper motions, in the case of active galactic nucleus (AGN) jets, systematic studies have been conducted using the technique of very long baseline interferometry (VLBI). It has been reported that the terminal velocities of the jets can reach up to a Lorentz factor (Γ) of ~ 30 based on Very Long Baseline Array (VLBA) 2 cm survey/MOJAVE samples (Kellermann et al. 2004; Lister et al. 2009). However, observational samples to address how and where jets are accelerated are still insufficient.

M87 is the one of the closest AGNs ($D = 16.7$ Mpc; Jordán et al. 2005) with a relativistic jet. At this distance, one milli-arcsecond (mas) corresponds to 0.084 pc, and 1 mas yr⁻¹ corresponds to 0.27 c . Thus, this enables us to measure a wide range of velocities from sub- to superluminal speeds using current VLBI techniques. In addition, since the mass of the central supermassive black hole is enormous ($3.2\text{--}6.6 \times 10^9 M_\odot$; Macchetto et al. 1997; Gebhardt et al. 2011; Walsh et al. 2013),⁴ the Schwarzschild radius (r_s) is 131 AU = 0.0078 mas. This provides a unique opportunity to explore a relativistic jet with the largest angular scale in terms of r_s .

At arcsecond scales, a one-sided jet has been detected from radio through optical to X-ray (e.g., Owen et al. 1989; Sparks et al. 1996; Perlman et al. 1999; Marshall et al. 2002). At the mas scale, the existence of the counter jet is reported with VLBA observations at 15 and 43 GHz (Ly et al. 2004; Kovalev et al. 2007; Walker et al. 2008), though the approaching side of the jet still dominates its emission. Very recently, the “central engine”

of M87 (probably indicating the position of the black hole and accretion disk) was determined, using phase-referenced VLBI observations, to be located only 21 μ s upstream from the VLBI core at 43 GHz in projected distance (Hada et al. 2011).

The proper motions of the M87 jet have been probed by VLBI for the innermost region ($<1''$ from the core), and by the Very Large Array (VLA) and the *Hubble Space Telescope* (HST) for the outer region ($>1''$ from the core) during the past two decades. VLBI observations at cm wavelengths have detected only subluminal ($<0.3 c$) or no proper motions within error (e.g., Reid et al. 1989; Dodson et al. 2006; Kovalev et al. 2007). The range of speeds were intensively measured with the VLBA at 15 GHz, and it was revealed that only very slow proper motions between 0.003 c to 0.05 c exist in the range from 1 to 20 mas from the nucleus (Kovalev et al. 2007). On the other hand, recent VLBA observations at 43 GHz claim to have detected very fast proper motions; 1.1 c or more at 0.5 mas (Acciari et al. 2009) and around 2 c in the range from 1 to 5 mas (Walker et al. 2008). These observed speeds are different from previous observations. We will discuss this discrepancy in Section 4.3.

HST observations have revealed trails of superluminal features at around $1''$ from the core (a region named HST-1) with a range of 4 c –6 c (Biretta et al. 1999). VLA and HST observations have detected both super- and subluminal motions downstream of HST-1 (Biretta et al. 1995; Meyer et al. 2013). Both the HST and VLA observations suggest a global trend that observed proper motions decrease smoothly as a function of the distance from HST-1.

To summarize the observed proper motions, an interesting picture has been derived thus far: no evidence for highly relativistic velocities between the core and HST-1, and then, suddenly, superluminal motion of components immediately on reaching HST-1. There is a missing link on the velocity field of the M87 jet between 160 and 900 mas. Exploring the velocity field on this spatial scale is the key to investigating the dynamics

⁴ Throughout the Letter, we adopt a black hole mass of $6.6 \times 10^9 M_\odot$.

Table 1
Results of the Model Fitting

Component	2007				2008				2009			
	<i>I</i>	<i>r</i>	P.A.	<i>d</i>	<i>I</i>	<i>r</i>	P.A.	<i>d</i>	<i>I</i>	<i>r</i>	P.A.	<i>d</i>
	(mJy) (1)	(mas) (2)	(degree) (3)	(mas) (4)	(mJy) (5)	(mas) (6)	(degree) (7)	(mas) (8)	(mJy) (9)	(mas) (10)	(degree) (11)	(mas) (12)
C7	0.071	185.2	−67.0	15.0	0.050	191.6	−66.9	16.8	0.047	190.3	−66.9	15.7
C6	0.047	241.2	−66.8	28.7	0.044	241.3	−66.6	30.2	0.050	256.2	−66.5	30.7
C5	0.039	276.1	−66.9	22.1	0.031	275.8	−66.7	23.9	0.024	287.5	−66.8	21.9
C4	0.060	308.0	−66.3	27.2	0.046	311.3	−66.3	28.4	0.056	314.7	−66.6	33.1
C3	0.026	342.0	−65.9	22.8	0.033	347.8	−66.1	26.1	0.034	362.0	−66.4	31.2
C2	0.062	378.1	−67.4	28.2	0.057	385.3	−67.8	32.2	0.040	398.8	−68.4	33.1
C1	0.029	411.8	−68.5	31.5	0.026	424.0	−67.9	42.0	0.016	442.4	−68.8	39.0

Notes. Columns are as follows: (1) total *I* flux density (mJy) for 2007, (2) position offset (mas) from the core component for 2007, (3) position angle (P.A.) with respect to the core component in degrees, (4) size of the fitted Gaussian (mas), (5)–(8) the same for 2008, (9)–(12) the same for 2009.

of the M87 jet and provides us with clues to understand the acceleration mechanism of the jet.

2. OBSERVATIONS AND DATA REDUCTION

We conducted monitoring observations of M87 on 2007 March 12, 2008 March 2, and 2009 March 7 using the European VLBI Network (EVN) and Multi-Element Radio Linked Interferometer Network at a wavelength of 18 cm. EVN observations were conducted with the Cambridge (UK), Effelsberg (Germany), Jodrell Bank (UK), Knockin (UK; only at last epoch), Medicina (Italy), Noto (Italy), Onsala (Sweden), Torun (Poland), and Westerbork (Netherlands) stations. Both left and right circular polarization data were recorded at each telescope using eight channels of 8 MHz bandwidth and 2 bit sampling. The data were correlated with the Joint Institute for VLBI correlator.

A priori amplitude calibration for each station was derived from a measurement of system temperatures during each run and the antenna gain. Fringe fitting was performed using the AIPS. After delay and rate solutions were determined, the data were averaged over 12 s in each intermediate frequency and self-calibrated using Difmap.

For the self-calibrated images, we performed model fitting using Difmap. The core is defined by Gaussian model fitting for the innermost bright region. Both of the circular or elliptical Gaussian models have been applied, but the relative position of each component with respect to the core is well determined. We summarize the results of the fitting in Table 1. After fitting, we cross-identified the components using not only their positions, but also their size and flux densities. The fitted size of the components agree from one epoch to the next when assuming less than 10% error for each measurement in most cases. The measured flux densities agree from one epoch to next when assuming less than 20% error for each measurement in most cases as well. Therefore, we think that our identification is robust.

3. RESULTS

We show the multi-epoch images from EVN observations in Figure 1. The bright core at the eastern edge of the jet and the continuous jet emission up to 500 mas from the core are clearly detected. The isolated component at a distance of 900 mas from the core corresponds to the HST-1 knot. The jet components between 160 mas to 500 mas have been suggested

by previous measurements (Cheung et al. 2007), but they are robustly detected and resolved with high significance in our EVN observations.

In Figure 1, green circles mark the model components for the jet structure by fitting circular Gaussians to the emission. Red lines represent their individual trajectories over time. We detect no proper motions within the first 160 mas from the core, while we detect significant superluminal motions of $2.5c$ and $3.5c$ for HST-1. These results are consistent with previous measurements (Dodson et al. 2006; Kovalev et al. 2007; Cheung et al. 2007). In addition to this, we detected proper motions of the components at a distance between 160 mas and 500 mas from the core for the first time, so the new data allow us to investigate the proper motions of this intermediate region down to HST-1.

Figure 2 shows the apparent velocity ($\beta_{\text{app}} = v_{\text{app}}/c$) for each jet component as a function of projected distance from the core, together with previous measurements over the innermost (Reid et al. 1989; Kovalev et al. 2007) and outermost regions (Cheung et al. 2007; Biretta et al. 1995, 1999). We also show the measurements by Ly et al. (2007), Walker et al. (2008), and Acciari et al. (2009). However, we do not use those measurements in the following discussion, as the errors are not given. We will discuss discrepancy of those measurements in Section 4.3. We identify the smooth transition in the proper motions from the sub- to superluminal regimes with a range of $0.67c \pm 0.63c$ to $3.74c \pm 1.18c$ in our EVN observations. The apparent velocity increases, and connects to the data points from previous measurements at both 160 mas and 900 mas. We capture a systematic increase of apparent proper motions from subluminal up to superluminal speeds peaking at around 900 mas, where the HST-1 complex is located. Beyond the HST-1 complex, the apparent velocities gradually decrease (Biretta et al. 1995, 1999; Meyer et al. 2013). Thus, our EVN observations fill in the missing link in the velocity distribution of the M87 jet, and they enable us to discuss the dynamics of the relativistic jet in this source by compiling observational data from over 20 yr.

4. DISCUSSION

4.1. Indication of Gradual Acceleration

In Figure 3 we show the velocity and its corresponding Lorentz factor for each jet component as a function of the deprojected distance from the core. We assume that the viewing angle of the jet is 14° based on beaming analysis (Wang & Zhou

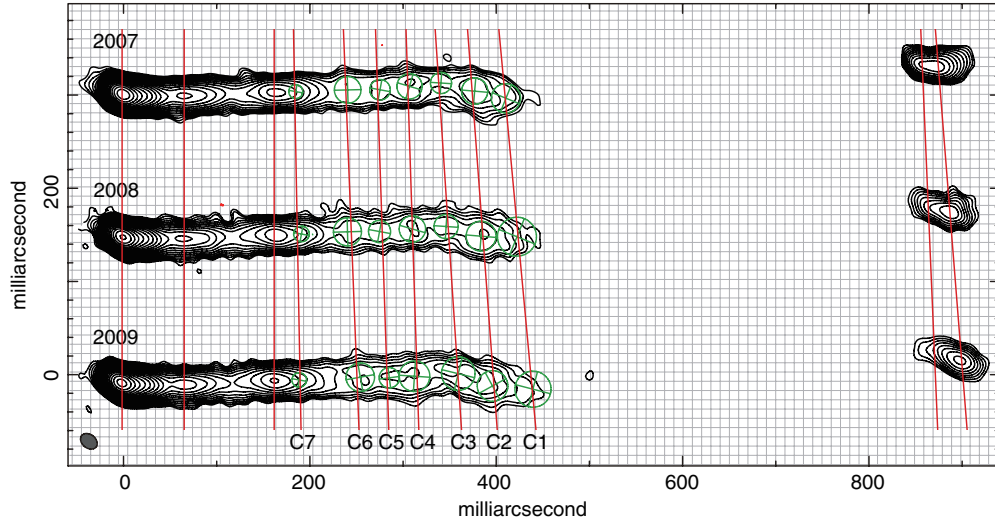


Figure 1. Contours are plotted at $-1, 1, 1.4142, \dots, 1024 \times 2.12 \text{ mJy beam}^{-1}$, which is three times the residual rms noise in the first epoch image. The synthesized beam is $19.9 \text{ mas} \times 14.6 \text{ mas}$ with the major axis at a position angle of 73.4° for the first epoch. Model components and trajectories are represented by green circles and red lines, respectively.

(A color version of this figure is available in the online journal.)

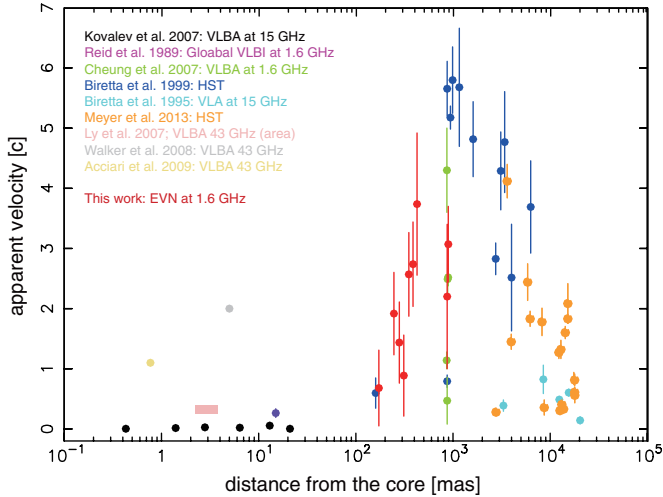


Figure 2. Distribution of the apparent velocity as a function of the projected distance from the core. Measurements by VLBA at 15 GHz (black circles), global VLBI at 1.6 GHz (purple circle), our measurements (red circles), VLBA at 1.6 GHz (green circles), *HST* (blue circles), VLA at 15 GHz (light blue circles). Error bars represent $\pm 1\sigma$. EVN points connect the subluminal speed measured toward the innermost jet with VLBA at 15 GHz and the superluminal speed measured toward *HST*-1 using *HST* and VLBA. We also plotted VLBA measurement at 43 GHz by Walker et al. (2008) and Acciari et al. (2009) as a reference. We also show the velocity measurements by Ly et al. (2007) as the area. Since their way of invoking the proper motion is different from the others and the error is not stated in their papers, we cannot include the error bar on those points. We consider these fast proper motions as a different phenomenon (see Section 4.3).

(A color version of this figure is available in the online journal.)

2009). We also assume that it does not change at all along the jet. We calculate a Lorentz factor $\Gamma = 1/(1-\beta^2)$ and velocity $\beta = \beta_{\text{app}}/(\sin\theta + \beta_{\text{app}} \cos\theta)$.

It is clear that both the velocity and the Lorentz factor in the intermediate region of our EVN measurements are connected to the inner and outer regions sampled in previous measurements. It is remarkable that the increase of the velocity from non-relativistic ($0.01 c$) to relativistic ($0.97 c$) speeds takes place over $10^{2-6} r_s$ in the deprojected distance from the core. If we

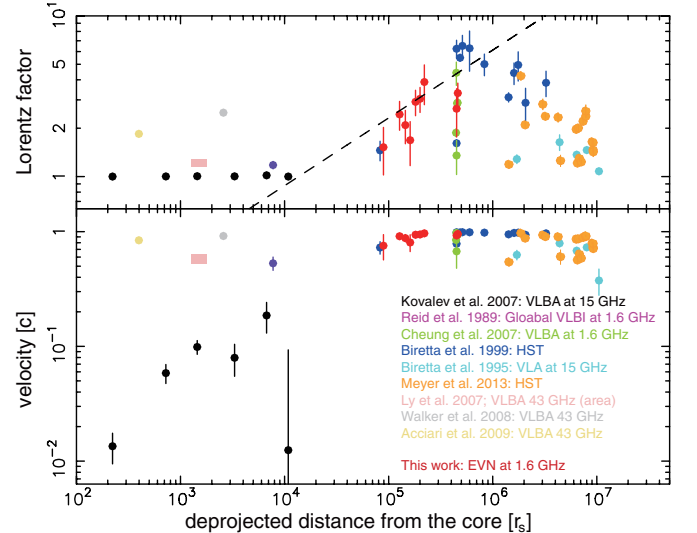


Figure 3. Distribution of the velocity and Lorentz factor as a function of the deprojected distance from the core. Measurements are illustrated in the same manner as in Figure 2. The dashed line represents the expected line, $\Gamma \sim z^{(b-1)/b}$, due to the MHD acceleration in parabolic streamline (e.g., Komissarov et al. 2009) with its power-law index $b = 1.7$ (Asada & Nakamura 2012). Deviation from the predicted line is large at the distance $< 10^4 r_s$, since the expected line is only applicable for relativistic regimes.

(A color version of this figure is available in the online journal.)

simply assume that the observed proper motions represent the speed of the bulk flows, the gradual acceleration of the bulk flow takes place from $200 r_s$ up to $5 \times 10^5 r_s$ over three orders of magnitude of the distance.

We note that a similar apparent acceleration has been observed in the jet of Cyg A from $0.2 c$ to $0.7 c$ at $2-10 \times 10^3 r_s$ (Krichbaum et al. 1998) and for NGC 315 from $1.1 c$ to $2.5 c$ at $5-20 \times 10^3 r_s$ (Cotton et al. 1999). However, these accelerations are seen in a limited range of the jets at around $10^3 r_s$. This is probably due to the sensitivity limit, and a limited part of the gradual acceleration of the jet is seen for those objects.

4.2. Comparison with the Structure of the Jet

In the general framework of asymptotic evolution of magnetohydrodynamic (MHD) jets in parabolic streamlines, both bulk acceleration and collimation take place simultaneously. The structure of the M87 jet has been intensively investigated with VLA/VLBA observations (e.g., Junor et al. 1999), which revealed that the jet changes its opening angle smoothly from 60° at ~ 0.03 pc to smaller than 10° over ~ 10 pc. This decrease of the opening angle is considered to be collimation (Junor et al. 1999). Since collimation is continuously occurring up to ~ 10 pc from the core, the MHD process was considered as the collimation mechanism (Junor et al. 1999). More recently, based on multi-frequency VLBI analysis, the M87 jet has been described as a parabolic streamline with a power-law index of 1.7; the collimation region has been identified to be between a few r_s to $10^6 r_s$ from the core, which is also the distance of HST-1 and close to the Bondi radius (Asada & Nakamura 2012; Nakamura & Asada 2013; Hada et al. 2013).

Nakamura & Asada (2013) suggest an acceleration of the M87 jet in the sub-relativistic regime on $10^{2-4} r_s$ by considering the magnetic nozzle effect. If this is the case, a continuous acceleration zone may presumably expand from a few r_s up to $10^6 r_s$, corresponding to the collimation zone in the M87 jet.

On the other hand, the velocity field newly revealed by the EVN observations captures a systematic acceleration of the jet in a mildly relativistic regime. In the framework of MHD jets in a fully relativistic regime, an acceleration of the jet can be expressed as a function of the distance z , associated with the parabolic stream line with a power-law index b , as $\Gamma \propto z^{(b-1)/b}$ (e.g., Komissarov et al. 2007, 2009). In the case of M87, the power-law index, b , is determined to be 1.7 (Asada & Nakamura 2012), so we would expect to see the acceleration of the jet as $\Gamma \sim z^{0.42}$. We show this power-law line in Figure 3 for reference. We do not perform fitting of it, since this equation is good for highly relativistic regimes ($\Gamma \gg 1$), while the velocity field revealed by EVN observations is a mildly relativistic regime. However, the measured proper motions show a similar tendency in the function of distance from the core.

Since the observed acceleration and collimation regions are co-spatial and the velocity fields are in good agreement with those expected for parabolic MHD jets in both non-relativistic (Nakamura & Asada 2013) and relativistic regimes (this Letter), we suggest that magnetic acceleration processes play a role in the dynamics of the M87 jet from $0.01 c$ (at $200 r_s$) up to $0.97 c$ (at $5 \times 10^5 r_s$). This acceleration and collimation zone would correspond to the entire region within the sphere of influence of the supermassive black hole, which is characterized by the Bondi radius.

It is suggested that a parabolic streamline is sustained in the M87 jet toward $< 10 r_s$ from the central engine (Nakamura & Asada 2013). If this is the case, similar magnetic acceleration is expected more toward the upper stream of the jet, so that future monitoring observations with sub-mm VLBI would be important for revealing an initial MHD acceleration together with identifying the footpoint of the jet.

4.3. Discrepancy of Proper Motions among VLBI Observations

There is a large discrepancy in observed proper motions between 15 and 43 GHz at the same region of 1–10 mas scales. The jet is optically thin in this region at 15 GHz and the widths of the jet are in good agreement with each other at 15 and 43 GHz (Asada & Nakamura 2012), so we would

speculate that the jet emissions come from almost the same layer. We reproduced two images obtained with VLBA at 43 and 15 GHz at close epochs in 2007 (January 27 at 43 GHz and February 5 at 15 GHz). We compared the two images by restoring the synthesized beam at 43 GHz with that at 15 GHz. The obtained images are quite similar to each other, and we can easily identify the bright knots inbetween the two images. Therefore, we naturally expect to see similar proper motions even at different frequencies. However, the VLBA observation at 43 GHz detected superluminal motions up to $2 c$, while VLBA and VLBI observations at the other frequencies including 15 GHz detected no or only slow subluminal motions (see also Figure 2).

Walker et al. (2008) explained this discrepancy by the difference of the sampling interval of observations. The fast motions observed at 43 GHz were detected only in plume-like components with an observational interval shorter than two weeks. Walker et al. (2008) pointed out that these plume-like components are short-lived, and an observational interval shorter than two weeks is required to fully trace these features. On the other hand, the sampling interval at 15 GHz is relatively sparse (every 2–8 months, 5 months in median) in comparison with that at 43 GHz (every 5 and 20 days). Due to the short life of the components with superluminal motions at 43 GHz, these motions would not be detected by current 15 GHz observations.

Kovalev et al. (2007) also considered the possibility of the existence of fast motions based on their 20 yr of monitoring, but conclude that fast motions are highly unlikely based on the four aspects which they mentioned, even with their sparse sampling interval. One possible explanation is that the detected fast proper motions can be interpreted as the bulk flow velocity (Walker et al. 2008), while the slow motions reflect standing shocks and/or pattern velocities associated with instabilities (Kovalev et al. 2007; Walker et al. 2008). However, this does not explain why we do not see different proper motions, so observationally this is still puzzling. We also note that the slow proper motions taken by VLBA 15 GHz increase as a function of distance from the core, and thus an interpretation as standing shocks may be inconsistent.

From the theoretical perspective, these observed subluminal motions can be explained by an MHD bulk velocity of the flow in a sub-relativistic regime (Nakamura & Asada 2013), while they have been interpreted during past decades as standing shocks and/or some pattern of plasma instability in supersonic jets (Kovalev et al. 2007; Walker et al. 2008). Moreover, the newly observed acceleration from sub- to superluminal motion is in good agreement with the observational evidence of gradual collimation up to $5 \times 10^5 r_s$, therefore it is straightforward to consider the slow motions as the velocity of the bulk flow. However, even if this is the case, the origin of the fast proper motions is unclear. It may be associated with some pattern velocity, or it may also be associated with the bulk velocity of the flow by considering multi-layers on the jet structure. If the proper motions observed at 43 GHz are associated with the bulk velocity of the flow, we can expect the components with faster proper motions further downstream of the jet to be accelerated with an MHD nozzle effect. However, current VLBI observations at low frequencies have not detected such motions. It would be necessary to conduct simultaneous VLBI observations at 15 and 43 GHz to solve this puzzle.

We thank P. T. P. Ho for stimulating discussions. K.A. thanks members of the Greenland Telescope Project for their warm

encouragement. The European VLBI Network is a joint facility of European, Chinese, South African, and other radio astronomy institutes funded by their national research councils.

Facilities: EVN, MERLIN, VLBA

REFERENCES

- Acciari, V. A., Aliu, E., Arlen, T., et al. 2009, *Sci*, **352**, 444
- Asada, K., & Nakamura, M. 2012, *ApJL*, **745**, L28
- Biretta, J. A., Sparks, W. B., & Macchetto, F. 1999, *ApJ*, **520**, 621
- Biretta, J. A., Zhou, F., & Owen, F. N. 1995, *ApJ*, **447**, 582
- Cheung, C. C., Harris, D. E., & Stawarz, Ł. 2007, *ApJL*, **663**, L65
- Cotton, W. D., Feretti, L., Giovannini, G., Lara, L., & Venturi, T. 1999, *ApJ*, **519**, 108
- Dodson, R., Edwards, P. G., & Hirabayashi, H. 2006, *PASJ*, **58**, 243
- Gebhardt, K., Adams, J., Richstone, D., et al. 2011, *ApJ*, **729**, 119
- Hada, K., Doi, A., Kino, M., et al. 2011, *Natur*, **477**, 185
- Hada, K., Kino, M., Doi, A., et al. 2013, *ApJ*, **775**, 70
- Jordán, A., Côté, P., Blakeslee, J. P., et al. 2005, *ApJ*, **634**, 1002
- Junor, W., Biretta, J. A., & Livio, M. 1999, *Natur*, **401**, 891
- Kellermann, K. I., Lister, M. L., Homan, D. C., et al. 2004, *ApJ*, **609**, 539
- Komissarov, S. S., Barkov, M. V., Vlahakis, N., & Königl, A. 2007, *MNRAS*, **380**, 51
- Komissarov, S. S., Vlahakis, N., Königl, A., & Barkov, M. V. 2009, *MNRAS*, **394**, 1182
- Kovalev, Y. Y., Lister, M. L., Homan, D. C., & Kellermann, K. I. 2007, *ApJL*, **668**, L27
- Krichbaum, T. P., Alef, W., Witzel, A., et al. 1998, *A&A*, **329**, 873
- Lister, M. L., Cohen, M. H., Homan, D. C., et al. 2009, *AJ*, **138**, 1874
- Ly, C., Walker, R. C., & Junor, W. 2007, *ApJ*, **660**, 200
- Ly, C., Walker, R. C., & Wrobel, J. M. 2004, *AJ*, **127**, 119
- Macchetto, F., Marconi, A., Axon, D. J., et al. 1997, *ApJ*, **489**, 579
- Marshall, H. L., Miller, B. P., Davis, D. S., et al. 2002, *ApJ*, **564**, 683
- Meyer, E. T., Sparks, W. B., Biretta, J. A., et al. 2013, *ApJL*, **774**, L21
- Nakamura, M., & Asada, K. 2013, *ApJ*, **775**, 118
- Owen, F. N., Hardee, P. E., & Cornwell, T. J. 1989, *ApJ*, **340**, 698
- Perlman, E. S., Biretta, J. A., Zhou, F., Sparks, W. B., & Macchetto, F. D. 1999, *AJ*, **117**, 2185
- Reid, M. J., Biretta, J. A., Junor, W., Muxlow, T. W. B., & Spencer, R. E. 1989, *ApJ*, **336**, 112
- Sparks, W. B., Biretta, J. A., & Macchetto, F. 1996, *ApJ*, **473**, 254
- Walker, R. C., Ly, C., Junor, W., & Hardee, P. J. 2008, *JPhCS*, **131**, 012053
- Walsh, J. L., Barth, A. J., Ho, L. C., & Sarzi, M. 2013, *ApJ*, **770**, 86
- Wang, C.-C., & Zhou, H.-Y. 2009, *MNRAS*, **395**, 301